IEEE Photonics Journal
An IEEE Photonics Society Publication

Accurate Chromatic Dispersion Characterization of Photonic Integrated Circuits

Volume 4, Number 3, June 2012

S. Mas
J. Matres
J. Martí
C. J. Oton

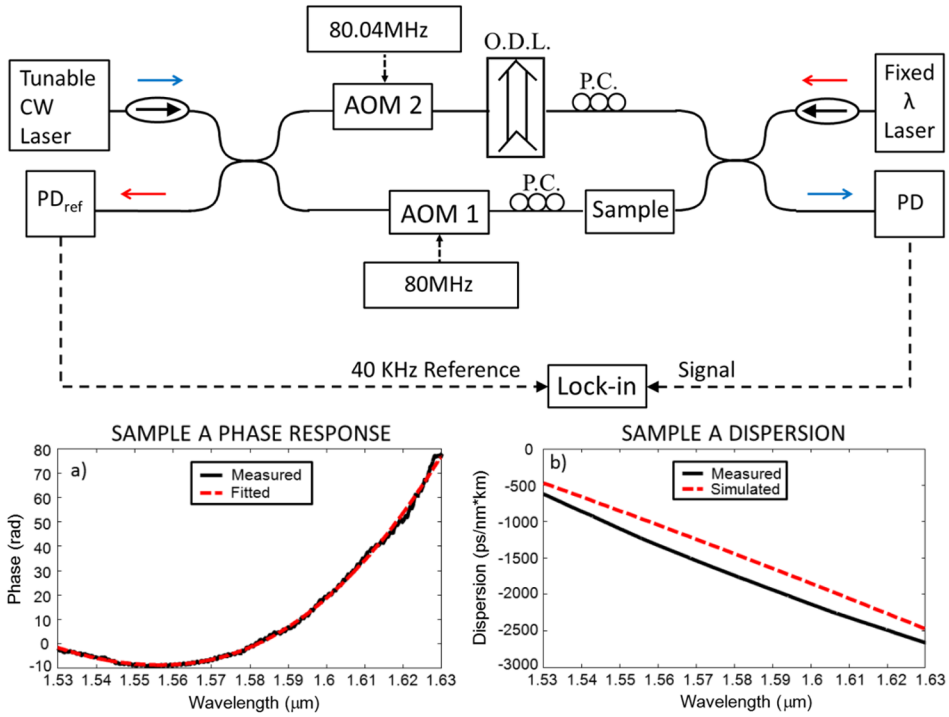

DOI: 10.1109/JPHOT.2012.2199294
1943-0655/$31.00 ©2012 IEEE

Accurate Chromatic Dispersion Characterization of Photonic Integrated Circuits

S. Mas, J. Matres, J. Martí, and C. J. Oton

Valencia Nanophotonics Technology Center, Universitat Politècnica de València, 46022 Valencia, Spain

DOI: 10.1109/JPHOT.2012.2199294
1943-0655/$31.00 ©2012 IEEE

Manuscript received March 23, 2012; revised May 5, 2012; accepted May 7, 2012. Date of current version May 22, 2012. This work was supported by the Spanish Ministry of Science and Innovation through contracts SINADEC (TEC2008- 06333) and DEMOTEC (TEC2008-06360), from Generalitat Valenciana through PROMETEO-2010-087 RD Excellence Program (NANOMET) and Universitat Politècnica de València through PAID-06-10 project 1914. Corresponding author: S. Mas (e-mail: smasg@ntc.upv.es).

Abstract: An accurate technique to characterize chromatic dispersion and its slope versus wavelength is reported. The method is based on a heterodyne Mach–Zehnder interferometer, which is immune to thermal phase noise by using a counterpropagating reference beam. Chromatic dispersion profiles are obtained over a broad wavelength region even in short waveguides with considerable loss. Conventional strip silicon waveguides as well as slotted geometries are considered. Theoretical simulations are also presented for comparison, which show good agreement with the experimental results.

Index Terms: Silicon nanophotonics, waveguides.

1. Introduction

Transporting and processing high bitrate signals require a precise management of dispersion properties [1], [2]. Nonlinear effects are also very sensitive to, not only dispersion, but its exact dependence with wavelength, i.e., its higher order derivatives [1]. Chromatic dispersion measurement techniques have been reported by many authors. Examples of these are techniques like time-of-flight [3] or phase-shift methods [4]. Time-of-flight methods are based on the relative temporal delays measurement for pulses at different wavelengths and, in phase-shift methods, the input to output phase shift of a modulated signal is measured in order to obtain the group delay spectra. These dispersion characterization techniques were originally conceived for optical fibers, where propagation distance can be made very long in order to provide large delays. When the sample to measure is short, more precise interferometric techniques are needed like the ones reported in [5]–[10]. These techniques employ a Mach–Zehnder interferometer (MZI) or Michaelson interferometer, where the fringe positions provide the phase information. However, interferometers, especially if fiber-based, suffer from thermal fluctuations which introduce phase noise that randomly shifts the fringes. If the insertion loss of the sample is high, the measurement may require several seconds or minutes, which is a timescale where thermal phase noise can dramatically degrade the measurement.

In other references [11]–[13], waveguide dispersion is measured by making a fully- integrated unbalanced MZI. Scanning the wavelength one can extract dispersion by measuring the change of free-spectral range (FSR) of the fringes. However, some problems of this technique are i) this only

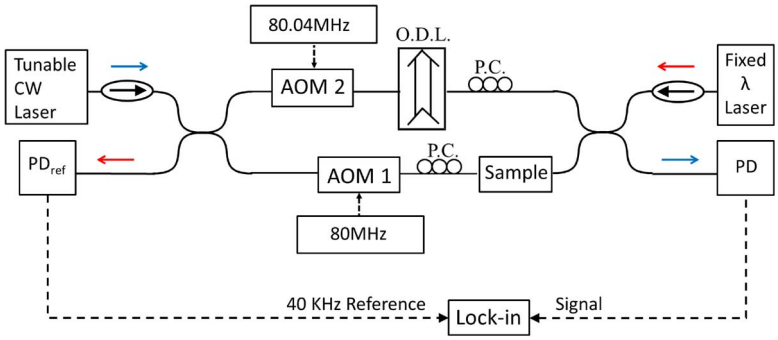

Fig. 1. Experimental setup. PC: Polarization controller, PD: Photo-detector, AOM: Acoustooptic modulator, ODL: Optical delay line. Solid lines denote fiber connections, and dashed lines, electrical connections. The ODL is pigtailed, but has a free-space delay inside. Isolators suppress the optical signals travelling toward the laser outputs.

provides discrete values of group index, ii) these measurements are also affected by thermal noise, and iii) the technique cannot be applied to a single straight waveguide, because an integrated MZI is needed.

In this paper, we propose a method for chromatic dispersion characterization with a fiber-based MZI using a technique which is immune to thermal phase noise. We describe how the proposed experimental setup compensates the fringe instability and we show continuous chromatic dispersion profiles obtained for different waveguide geometries together with theoretical calculations.

2. Technique

Fig. 1 shows the measurement apparatus. It is a fiber-based MZI, where one of the branches has an optical delay line (ODL), and the other has the waveguide sample. Acoustooptic modulators (AOMs) are also present in both branches, and they are used as frequency shifters. Their RF frequencies are set to 80 and 80.04 MHz, respectively, so that when the beams are recombined they produce 40 kHz beatings which can be precisely measured with a lock-in amplifier. The lock-in also extracts the phase of the beatings, which is measured with respect to the phase of the beatings produced by a counterpropagating beam. This is carried out by amplifying the signal from the reference photodiode and sending it to the lock-in reference input. In this way, thermal fluctuations which affect both beams are cancelled out, and only the wavelength dependence of the phase is extracted during the sweep. A similar concept for stabilizing a MZI was reported in [14] for a distributed fiber sensor system. In principle, one could also use a copropagating beam as a reference, but that would require filters to separate the signal from the reference beam, thus a counterpropagating reference is easier to implement. On the other hand, if the lock-in amplifier in use can reach the MHz range, only one AOM would be necessary, as the beatings would have 80 MHz frequency.

Let us obtain the equations that govern the phase response of this system. Frequency dependent propagation constant can be expanded in Taylor series as follows [15]:

$$\beta(\omega) = n_{eff}(\omega)\frac{\omega}{c} = \beta_0 + \beta_1(\omega-\omega_0) + \frac{1}{2!}\beta_2(\omega-\omega_0)^2 + \frac{1}{3!}\beta_3(\omega-\omega_0)^3 + \ldots \quad (1)$$

where $\beta_i = (d^i\beta/d\omega^i)_{\omega=\omega_0}$ $(\mathrm{i} = 0, 1, 2\ldots)$. The first three terms of the propagation constant can be expressed as

$$\beta_0 = \frac{\omega_0}{c}n_{eff}(\omega_0), \quad \beta_1 = \frac{n_g(\omega_0)}{c}, \quad \beta_2 = \frac{-\lambda^2}{2\pi c}D_\lambda \quad (2)$$

where n_{eff} is the effective index, β_1 is related to the group index (n_g) and β_2 is the group velocity dispersion (GVD) parameter. Let us consider a MZI consisting of an homogeneous waveguide in one arm and a variable air path, e.g., an ODL, in the other branch. To compensate for the response

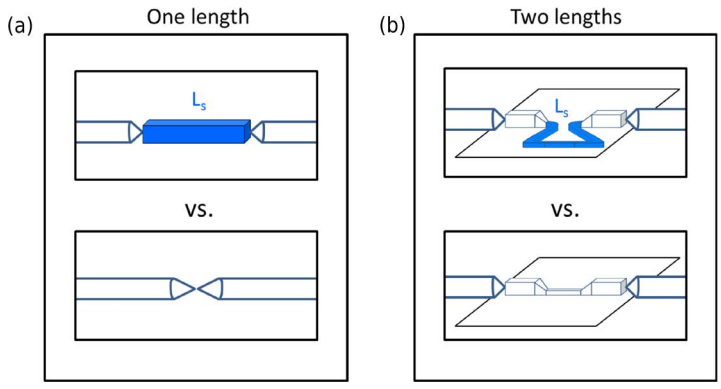

Fig. 2. Different measurement schemes, where the actual measurement is shown in the top panel and the reference in the bottom panel. (a) Only one length of homogeneous waveguide using a measurement with no sample as reference. (b) Two different lengths of a waveguide, using the shorter one as the reference.

of the system, two measurements with different lengths are necessary, the shortest one to be used as a reference. There are two possibilities to make this, as shown in Fig. 2. If the waveguide is homogeneous (no tapers or wider parts to facilitate the coupling) one can remove the sample to get the reference response [see Fig. 2(a)]. On the other hand, if the waveguide has section variations of considerable length, the reference must contain the same section variations, and only the length of the section under test must be different, as shown in Fig. 2(b).

In any case, we are interested in the phase difference with respect to the reference measurement, therefore the dispersion response of the AOMs, fibers, and waveguide coupling regions are all compensated. The response will only depend on L_s, which is the extra waveguide length between both measurements, and L_a, which is the extra air path added to the ODL to keep the MZI balanced.

If we define ϕ_s as the phase added when increasing the waveguide length by L_s and ϕ_a as the phase added when increasing the ODL path by L_a, we have

$$\phi_s(\omega) - \phi_s(\omega_0) = L_s\left(\beta_1\Delta\omega + \frac{\beta_2}{2!}\Delta\omega^2 + \frac{\beta_3}{3!}\Delta\omega^3\right) \tag{3}$$

$$\phi_a(\omega) - \phi_a(\omega_0) = L_a\frac{\Delta\omega}{c}. \tag{4}$$

Hence, the phase difference between both branches $\Delta\phi = \phi_s - \phi_a$ is given by

$$\Delta\phi(\omega) - \Delta\phi(\omega_0) = \left(L_s\beta_1 - \frac{L_a}{c}\right)\Delta\omega + L_s\left(\frac{1}{2!}\beta_2\Delta\omega^2 + \frac{1}{3!}\beta_3\Delta\omega^3\right). \tag{5}$$

Balancing the MZI consists of adjusting L_a to make the first term in $\Delta\omega$ equal to zero. This is experimentally carried out by moving the ODL until the slope of the phase at the central wavelength becomes zero. Under these conditions, the group index of the waveguide under test will be given by

$$n_g = c\cdot\beta_1 = \frac{L_a}{L_s}. \tag{6}$$

The ODL must have a range which is long enough to cover the path difference between the reference sweep and the signal sweep. An ODL range of 500 ps would allow the characterization of devices up to that amount of delay, which corresponds to an approximate length of 37 mm (assuming a group index of 4), which is enough for most photonic integrated circuits.

Once the MZI is balanced, the terms from (5) in $\Delta\omega^2$ and $\Delta\omega^3$ can be obtained from a polynomial fit of the resulting curve. In principle, one could also obtain higher-order dispersion terms, but these

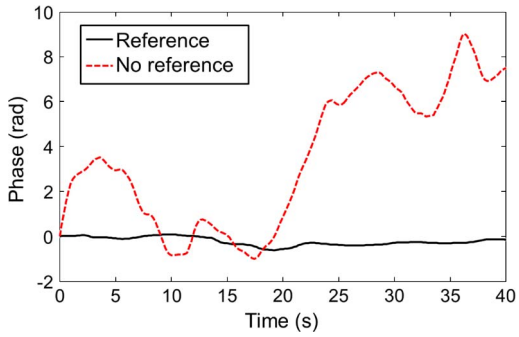

Fig. 3. Phase noise versus time when the measurement is unreferenced (red, dashed) and referenced with a counter-propagating beam at fixed wavelength (black, solid). Signal and reference wavelengths were 1550 and 1530 nm, respectively. The phase noise is dramatically reduced by referencing.

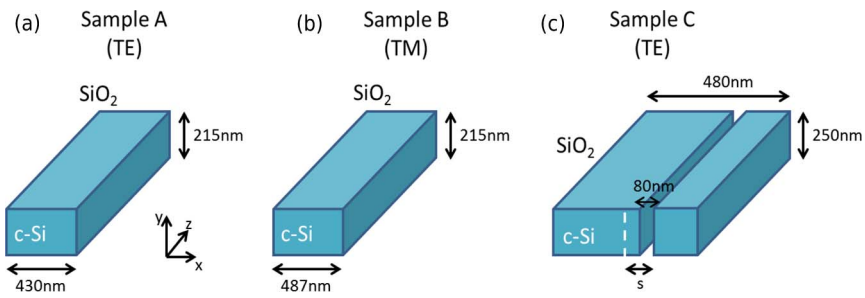

Fig. 4. Different measured waveguides. (a) 430 nm wide silicon strip for TE polarization. (b) 487 nm wide silicon strip for TM polarization. (c) Vertical slot waveguide. Waveguide parameters were extracted from SEM micrographs and were fine-tuned within the measurement error range to optimize the fitting.

terms would only become evident if lower-order terms are small. In our case, we have fitted the curves up to third-order.

Fig. 3 shows the effect of thermal phase drift. The red dashed curve shows the fluctuations of the signal beam phase with time without using the counterpropagating beam as a reference. In this case, the lock-in amplifier was referenced with the 40 kHz beatings obtained from mixing the RF sources of the AOMs. The plot shows a noise level which would prevent a reliable measurement of the phase dependence on wavelength with a sweep that takes several seconds. On the other hand, the solid black curve shows the phase when referencing with the beatings produced by the counterpropagating reference beam. The fixed wavelength of the counterpropagating beam must be close to the propagating signal wavelength, as this way the phase noise is reduced to the minimum. For this reason, it was set to the central wavelength where the MZI is balanced. The phase noise is greatly reduced because thermal fluctuations of the optical paths of both branches equally affect both beams.

3. Fabrication

In this paper, we show the characterization of silicon-based waveguides with three different geometries, which we call Sample A, B and C.

Sample A and Sample B are strip waveguides patterned with deep-UV lithography. They have 2 μm oxide buffer, 25 mm length, and 215 nm height, as shown in Fig. 4(a) and (b). Sample A corresponds to a TE polarization channel waveguide with 430 nm width. Sample B, used as TM polarization channel waveguide, has 487 nm width. The sidewall angle introduced in the manufacturing process is 8° and 6° for Sample A and Sample B, respectively. These parameters were extracted from SEM micrographs, and were fine-tuned within the experimental error range to optimize the fitting. Sample C is a 50% asymmetric slot waveguide patterned with electron-beam lithography. It has 3 μm oxide

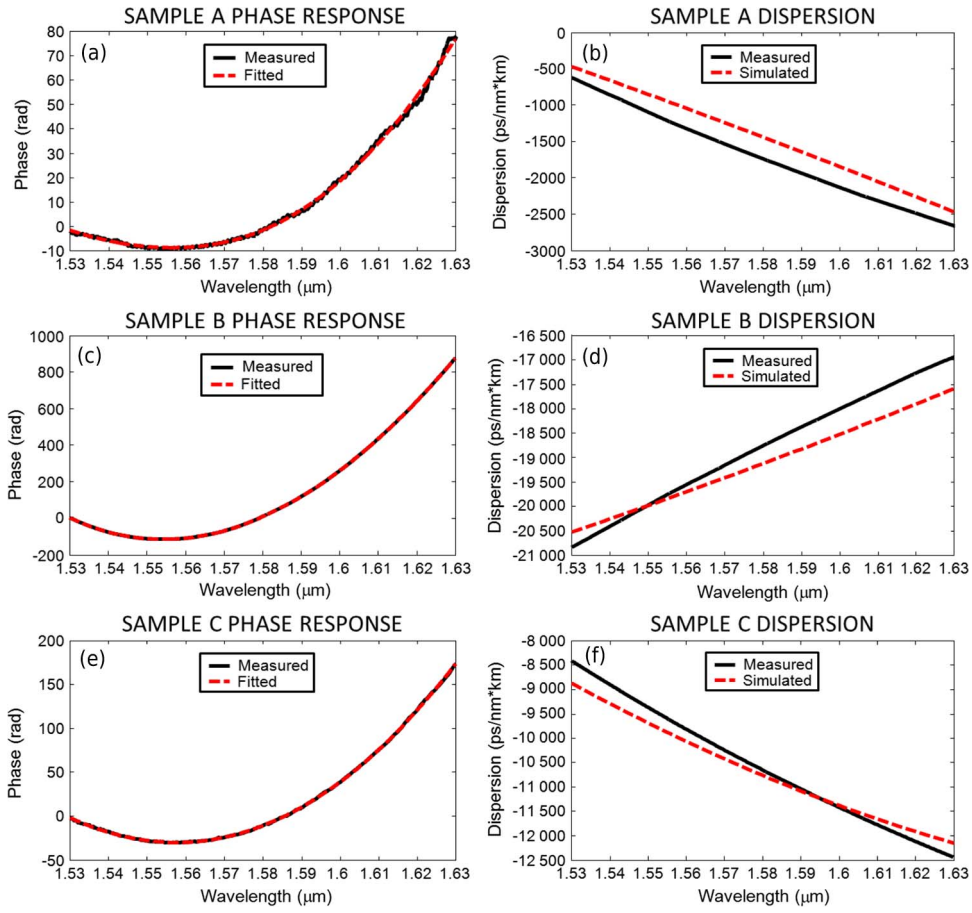

Fig. 5. Phase evolution and chromatic dispersion profiles for (a)–(b) TE polarization strip waveguide (Sample A), (c)–(d) TM polarization strip waveguide (Sample B) and (e)–(f) vertical slot waveguide (Sample C).

buffer, 14 mm length, and 250 nm height. In asymmetric slot waveguides, the slot location is different than the geometrical center of the waveguide. We define the asymmetry degree as $2s/w$ [16], where s is the distance from the center of the waveguide to the center of the slot, in absolute value, and $w/2$ is half of the total width of the waveguide, see Fig. 4(c). The waveguide consists of a 80 nm wide silica slot between two silicon rails with 5.5° angled sidewalls. All samples are covered with silica using plasma-enhanced chemical vapor deposition (PECVD).

In samples A and B light was vertically coupled through 70 nm-deep grating couplers. Total insertion loss was 24 dB for Sample A (TE) and 15 dB for Sample B (TM). On the other hand, for Sample C light was horizontally coupled using lensed fibers; total insertion loss was 54 dB.

4. Results

Fig. 5(a) and (c) show the phase experimental measurement and its polynomial fit for Sample A and Sample B, respectively. From the fit for each sample, chromatic dispersion profiles are obtained, Fig. 5(b) and (d), where numerical simulations performed by using commercial software based on finite element method are also presented for comparison. In theoretical calculations, we compute the effective index, $n_{eff}(\lambda)$, in a broad spectral range and by numerical differentiation the GVD parameter as a function of wavelength is obtained as $D_\lambda = -(\lambda/c)d^2 n_{eff}/d\lambda^2$. Material dispersion has been taken into account by considering the Sellmeier equation for both silicon and silica [17].

It can be seen that dispersion values and their slopes reasonably agree with the calculations; the small discrepancies are attributed to geometrical deviations of the fabricated device with respect to the simulation, which is assumed to be perfectly symmetric and homogeneous. In principle, there is no limitation on the dispersion measurable range. However, the minimum measurable dispersion would be determined by the phase noise, which depends on the experimental conditions. β_3 parameter is also obtained for both samples; for Sample A, we found an experimental value of $\beta_3 = -0.0394$ ps^3/m and a theoretical value of $\beta_3 = -0.0392$ ps^3/m. In the case of Sample B, experimental $\beta_3 = 0.019$ ps^3/m and calculated $\beta_3 = 0.0076$ ps^3/m values are obtained. Experimental group index values are 4.36 and 3.21 for TE polarization strip and TM polarization strip, respectively, while calculated values are 4.35 and 3.46, showing a good agreement too. Vertical slot waveguide experimental phase and its fitting are shown in Fig. 5(e). Fig. 5(f) shows the chromatic dispersion profile for this sample which presents a measured value of $\beta_3 = -0.0939$ ps^3/m and a calculated value of $\beta_3 = -0.0886$ ps^3/m. Experimental and theoretical values of group index for Sample C are 4.17 and 4.15, respectively.

5. Conclusion

A novel method for chromatic dispersion measurement in nanophotonic waveguides is proposed and demonstrated. By measuring the phase evolution versus wavelength of the waveguides in a MZI, the chromatic dispersion and its slope can be determined. The technique is immune to fringe instability and allows the characterization of integrated waveguides with high insertion loss. We have performed an accurate dispersion characterization of conventional strip waveguides for both TE and TM polarizations as well as vertical slot waveguide. The experimental results were in close agreement with those obtained from simulation.

Acknowledgment

We acknowledge D. Heinis for fruitful discussions.

References

[1] I. Walmsley, L. Waxer, and C. Dorrer, "The role of dispersion in ultrafast optics," *Rev. Sci. Instrum.*, vol. 72, no. 1, pp. 1–29, Jan. 2001.
[2] L. Zhang, Q. Lin, Y. Yue, R. G. Beausoleil, and A. E. Willner, "Silicon waveguide with four zero-dispersion wavelengths and its application in on-chip octave-spanning supercontinuum generation," *Opt. Exp.*, vol. 20, no. 2, pp. 1685–1690, Jan. 2012.
[3] L. Cohen and C. Lin, "A universal fiber-optic (UFO) measurement system based on a near-IR Raman laser," *IEEE J. Quantum Electron.*, vol. QE-14, no. 11, pp. 855–859, Nov. 1978.
[4] J. Hult, R. S. Watt, and C. F. Kaminski, "Dispersion measurement in optical fibers using supercontinuum pulses," *J. Lightw. Technol.*, vol. 25, no. 3, pp. 820–824, Mar. 2007.
[5] L. Thevenaz, J. P. Pellaux, and J. P. Von Der Weid, "All-fiber interferometer for chromatic dispersion measurements," *J. Lightw. Technol.*, vol. 6, no. 1, pp. 1–7, Jan. 1988.
[6] H. T. Shang, "Chromatic dispersion measurement by white-light interferometry on metre-length single-mode optical fibres," *Electron. Lett.*, vol. 17, no. 17, pp. 603–605, Aug. 1981.
[7] J. Y. Lee and D. Y. Kim, "Versatile chromatic dispersion measurement of a single mode fiber using spectral white light interferometry," *Opt. Exp.*, vol. 14, no. 24, pp. 11 608–11 615, Nov. 2006.
[8] H. K. Tsang, C. S. Wong, T. K. Liang, I. E. Day, S. W. Roberts, A. Harpin, J. Drake, and M. Asghari, "Optical dispersion, two-photon absorption and self-phase modulation in silicon waveguides at 1.5μm wavelength," *Appl. Phys. Lett.*, vol. 80, no. 3, pp. 416–418, Jan. 2002.
[9] C. Turner, C. Manolatou, B. S. Schmidt, M. Lipson, M. A. Foster, J. E. Sharping, and A. L. Gaeta, "Tailored anomalous group-velocity dispersion in silicon channel waveguides," *Opt. Exp.*, vol. 14, no. 10, pp. 4357–4362, May 2006.
[10] W. Ding, C. Benton, A. V. Gorbach, W. J. Wadsworth, J. C. Knight, D. V. Skryabin, M. Gnan, M. Sorrel, and R. M. De la Rue, "Solitons and spectral broadening in long silicon-on-insulator photonic wires," *Opt. Exp.*, vol. 16, no. 5, pp. 3310–3319, Mar. 2008.
[11] E. Dulkeith, F. Xia, L. Schares, W. M. J. Green, and Y. A. Vlasov, "Group index and group velocity dispersion in silicon-on-insulator photonic wires," *Opt. Exp.*, vol. 14, no. 9, pp. 3853–3863, May 2006.
[12] Y. A. Vlasov, M. OBoyle, H. F. Hamann, and S. J. McNab, "Active control of slow light on a chip with photonic crystal waveguides," *Nature*, vol. 438, pp. 65–69, Nov. 2005.
[13] D. T. H. Tan, K. Ikeda, P. C. Sun, and Y. Fainman, "Group velocity dispersion and self phase modulation in silicon nitride waveguides," *Appl. Phys. Lett.*, vol. 96, no. 6, pp. 61101-1–61101-3, Feb. 2010.

[14] J. Snoddy, Y. Li, F. Ravet, and X. Bao, "Stabilization of electro-optic modulator bias voltage drift using a lock-in amplifier and a proportional-integral-derivative controller in a distributed Brillouin sensor system," *Appl. Opt.*, vol. 46, no. 9, pp. 1482–1485, Mar. 2007.
[15] G. P. Agrawal, *Nonlinear Fiber Optics,* 3rd ed. New York: Academic, 2001.
[16] S. Mas, J. Caraquitena, J. V. Galán, P. Sanchis, and J. Martí, "Tailoring the dispersion behavior of silicon nanophotonic slot waveguides," *Opt. Exp.*, vol. 18, no. 20, pp. 20 839–20 844, Sep. 2010.
[17] B. Tatian, "Fitting refractive-index data with the Sellmeier dispersion formula," *Appl. Opt.*, vol. 23, no. 24, pp. 4477–4485, Dec. 1984.